Comparison of Methods for Generating Planar DNA-Modified Surfaces for Hybridization Studies

Amal Kasry,[†] Paola Borri,[†] Philip R. Davies,[‡] Adrian Harwood,[†] Nick Thomas,[§] Stefan Lofas,[||] and Trevor Dale*[,†]

Cardiff School of Biosciences, Biomedical Science Building, Museum Avenue, Cardiff CF10 3AX, U.K., Cardiff School of Chemistry, Park Place, Cardiff CF10 3AT, U.K., GE Healthcare, Maynard Centre, Whitchurch, Cardiff CF14 7YT, U.K., and GE Healthcare, Biacore AB, SE-75450 Uppsala, Sweden

ABSTRACT The surface conformation and accessibility of oligonucleotides within arrays are two key parameters that affect the utility of immobilized nucleic acids in sensor technologies. In this work, a novel combination of analytical techniques was used to compare two methods for DNA immobilization on glass. The aim of the study was to identify a method that generated a high surface density of hybridization-accessible oligonucleotides in a true planar monolayer. The first method based on direct coupling of silanized DNA to the glass surface showed a high immobilization density of 0.013 molecules/nm^2 but low surface accessibility, as shown by the hybridization measurements (≤15%). The second method, based on the biotin−streptavidin interaction, generated a high immobilization density (0.02 molecules/nm^2) and high surface accessibility (90%). Atomic force microscopy and X-ray photoelectron spectroscopy indicated that both methods achieved uniform surfaces. Using the biotin−streptavidin system, the intermolecular distance between the hybridized molecules could be tightly controlled by titrating biotinylated complementary and noncomplementary oligonucleotides.

KEYWORDS: biochips • DNA immobilization • DNA hybridization • surface accessibility • intermolecular distance control • fluorescence imaging

INTRODUCTION

Reproducible methods for DNA immobilization are central to a range of important technological applications. These techniques include, but are not limited to, analyses of gene expression using microarrays (1, 2), chromatin structure using immunoprecipitation (ChIP) (3), and DNA copy number determination (4, 5). These applications have encouraged detailed studies of surface modification methods [reviewed by Zhao (2008) and Xu (2007) (6, 7)]. Techniques for DNA immobilization are highly dependent on the nature of the substrates, which include gold, silicon, or glass. Gold is frequently used to immobilize thiol-modified oligonucleotides (8−12) based on the strong interaction between the sulfur group and the gold surface, leading to a high density of immobilized DNA (0.11 molecules/cm^2 (13)). However, glass surfaces are preferable in a range of applications because of their transparency, low fluorescence background, and physical rigidity. Glass is also amenable to various chemical modifications based on silanization chemistry. Silane analogues are used to create a monolayer surface with chemical reactivity that covalently couples to modified oligonucleotides. For example, mercaptosilanes can be used to couple thiol-modified oligonucleotides (14, 15), while epoxysilane- and carboxysilane-activated glass surfaces can be used to immobilize amino-modified oligonucleotides (16, 17). Last, aminosilane-treated surfaces can be directly coupled to aldehyde-modified oligonucleotides or can be indirectly coupled via spacer molecules such as *p*-phenylene-1,4-diisothiocyanate, which converts the support's primary amines to amino-reactive phenylisothiocyanate groups (18, 19). Direct immobilization can also be carried out by using directly silanized DNA (20).

The key features of DNA-modified surfaces are DNA density and hybridization accessibility. Most published immobilization methods achieve a good surface density, but surface conformation and surface accessibility are less frequently characterized. In many cases, high surface densities are intentionally generated by accessing the "*z* dimension". For example, branched surface-projecting dendrimers allow very high "surface" densities when projected as a hypothetical two-dimensional surface representation (21, 22). In other cases, the *z* dimension may be inadvertently accessed through the formation of sol gels during glass modification. While high surface densities are reported for these surfaces, many of the sites are inaccessible for hybridization.

Several methods have been enormously used to characterize DNA interfacial immobilization. These methods include optical spectroscopy methods like surface plasmon resonance (23), ellipsometry (24), X-ray photoelectron spectroscopy (XPS) (25), and fluorescence microscopy (26); these

* To whom correspondence should be addressed. Telephone: +44 (0)29 208 74652. Fax: +44(0)2920874116. E-mail: daletc@cf.ac.uk.
Received for review May 8, 2009 and accepted July 17, 2009
[†] Cardiff School of Biosciences. E-mail: kasrya@cf.ac.uk (A.K.), borrip@cf.ac.uk (P.B.), harwoodaj@cf.ac.uk (A.H.).
[‡] Cardiff School of Chemistry. E-mail: daviespr@cf.ac.uk.
[§] GE Healthcare, Maynard Centre. E-mail: nick.thomas@ge.com.
[||] GE Healthcare, Biacore AB.
DOI: 10.1021/am9003073

Table 1. DNA Sequences

name	sequence
	5′3′
Thio-Target	thiol · · · GCTCAGCACCAGGTGACTGGGTGACTTCAG · · · Atto488
Radio-Target	thiol · · · GCTCAGCACCAGGTGACTGGGTGACTTCAG
Thio-Probe	thiol · · · GCTCAGCACCAGGTGACTGGGTGACTTCAG
Biotin-Target	biotin · · · GCTCAGCACCAGGTGACTGGGTGACTTCAG · · · Atto488
Probe1	biotin · · · GCTCAGCACCAGGTGACTGGGTGACTTCAG
Probe2	biotin · · · CGAGTCACCTGTCACGGTGCCCAGTAAGTC
Target	Atto488 · · · CTGAAGTCACCCAGTCACCTGGTGCTGAGC
Control Oligo	Atto488 · · · GCTCAGCACCAGGTGACTGGGTGACTTCAG

methods can quantify the surface density but do not give enough information about conformation. Other methods like atomic force microscopy (AFM) can reveal the surface structure with high resolution (27). In most studies, a subset of these techniques are used to characterize DNA surfaces.

In the current study, we aimed to identify a method that generated planar DNA-modified surfaces with a high density of hybridization-accessible oligonucleotides. To reveal as much information as possible, an orthogonal mix of techniques including AFM, XPS, radioactive measurements, fluorescence imaging, and fluorescence spectroscopy were used to assess the surface density, structure, and accessibility. Two commonly used methods for immobilization of DNA oligonucleotides were compared. The first method involved the coupling of silanized DNA directly to the glass surface; this method showed a high surface density but resulted in poor surface accessibility. The second method involved the coupling of biotinylated DNA through a biotin–streptavidin-modified surface; this method generated an optimal surface structure with both a high surface density and hybridization accessibility. Importantly, this surface approximated a planar monolayer surface that was not multilayered or rough at the nanoscale.

EXPERIMENTAL METHODS

Preparation Procedures. Glass coverslips from Fisher Scientific were cleaned by sonication in Milli-Q water for 20 min followed by sonication in ethanol for 20 min, dried with nitrogen, and kept under nitrogen until use. Areas to be modified were defined by overlaying of the slides with a silicon gasket (Stratech Scientific, Newmarket Suffolk, U.K.) containing 50 wells of 3 mm diameter and 1 mm depth.

Silanized DNA Method. Silanized DNA was obtained by mixing 50 μM thiol-modified DNA (Thio-Target; Table 1) and 250 μM (3-mercaptopropyl)trimethoxysilane from Sigma-UK (in a ratio of 1:5) for 10 min at room temperature according to the protocol described in ref 20. The mixture was applied to the surface for 15 min. Unbound material was removed by washing with 30 mM sodium acetate (pH 4.3) for 2 min and by dipping in boiling water for 30 s. Coverslips were dried with nitrogen for storage if necessary.

Biotin–Streptavidin System. The glass surface was amino-modified by incubation in 2.4 mM (aminopropyl)triethoxysilane (APTES), from Sigma-UK, for 1 h at room temperature; the APTES solution was prepared using toluene as the solvent. The incubation was followed by three washes in toluene and one in Milli-Q water. The amino groups were coupled to biotin by incubation in 1.4 mM NHS–biotin (Sigma-UK) for 1 h at room temperature; the NHS–biotin was prepared using dimethyl sulfoxide (DMSO) as the solvent. This was followed by three washes in DMSO and one in Milli-Q water to remove any DMSO traces. Binding of streptavidin (from Roche Diagnostics) was carried out by incubation in 1 μM streptavidin for 30 min followed by washing with phosphate-buffered saline (PBS), containing 0.0027 M KCl and 0.137 M NaCl. Biotinylated DNA oligonucleotides (Table 1; at 50 nM unless otherwise stated) were applied to the surface for 30 min before washing with PBS. All of the DNA sequences were purchased from Biomers.net (Ulm, Germany).

Hybridization. Oligonucleotides labeled with γ^{32}P ATP (Perkin-Elmer) for radioactive measurements or with the Atto 488 fluorophore for the fluorescence imaging were hybridized to complementary oligonucleotide-coupled surfaces at a final concentration of 500 nM for times as described in the text. The sequences of the oligonucleotides used are shown in Table 1. Following hybridization unbound material was washed away with three washes in PBS.

Surface Characterization. ***AFM.*** Samples were imaged by AFM using a Veeco multimode atomic force microscope in air at room temperature. Phosphorus n- doped silicon tips were used for scanning in the tapping mode to avoid physical damage to the surface. AFM images were recorded for, at least, three different surface positions to check the surface uniformity. The images were analyzed using WSxM software (28), and the root-mean-square (rms) roughness was calculated for all of the images. Surface rms roughness is defined as the standard deviation of the heights in nanometers in the *XYZ* three-dimensional AFM map.

XPS. XPS analysis was performed with a Kratos Axis Ultra-DLD XPS system with a monochromated Al Kα source. XPS data were analyzed using Casa XPS software, where the surface density of the elements was quantified by calculating the area of the peak at the element's binding energy (29).

Radioactive Measurements. Trace levels (400 nM) of oligonucleotides were labeled with γ^{32}P ATP (Perkin-Elmer) by incubation with polynucleotide kinase according to the standard KinaseMax (Ambion) protocol. Labeled oligonucleotides were purified from unincorporated ATP using a Sephadex TM G-50 column and mixed with unlabeled oligonucleotides at an 80 μM final concentration in the surface modification studies and at a final concentration of 1 μM for hybridizing oligonucleotides (see the text for details). Quantification of the radioactive signal was measured in an LS 6500 multipurpose scintillation counter.

Fluorescence Measurements. Fluorescently labeled surfaces were imaged with an inverted microscope (Olympus IX71) equipped with a 10× objective (0.3 NA). A 490 nm filter (from Chroma) was used to define the wavelengths for fluorescence excitation, and a 520 nm filter was used in the emission path. The images were collected using a Hamamatsu high-resolution digital camera (ORCAAG) and analyzed by Image-j software. All images were collected for an area of 258 μm × 322.5 μm. Surfaces were also characterized with a time-correlated single photon counting (TCSPC) set up with optical excitation in the total internal reflection (TIR) mode, having a 90 nm evanescent field decay length, as 1/e of the maximum field intensity. TIR fluorescence was used to measure the surface hybridization in real time. TCSPC was performed using a laser source providing ~50 ps pulses at a 20 MHz repetition rate at 473 nm wavelength (Becker & Hickl GmbH) and photon counting electronics (SPC-150, Becker & Hickl GmbH) connected to a cooled photomultiplier (Hamamatsu H7422P-40). The time resolution of the system was ~250 ps. A 1.42 NA objective (from Olympus) was used to excite at TIR and collect the fluorescence signal. A mirror in a Gimbal mount allowed adjustment of the light incident angle without changing the position of the spot onto the sample. The fluorescence signal was collected over a typical integration time of 30 s. This setup was designed to measure the lifetime of fluorescently labeled oligonucleotides; however, in this work, it was only used to collect the fluorescence surface signal.

Measurements were performed in a rectangular flow cell built of a quartz glass slide and a poly(dimethylsiloxane) gasket with the dimensions of 15.94 mm length, 4.88 mm width, and 300 μm depth and with an inlet and an outlet at each end.

Calculation of the Surface Density and Intermolecular Distance. For radioactive measurements, the number of surface-bound molecules was calculated by comparing the sample coverslips with a standard curve of labeled oligonucleotides that had been dried onto coverslips. For fluorescence imaging, samples were uniformly illuminated and imaged using an epifluorescent microscope. Bulk solutions of fluorophore-labeled oligonucleotides of known concentration were used to produce a series of projected surface "densities" as references. Incubation of fluorophore-modified surfaces with PBS did not significantly alter the fluorescent signal (data not shown). From the ratio between the fluorescence intensity of the surface and the intensity of the reference bulk solution, the surface density was deduced and accordingly the mean distance between the DNA molecules calculated according as

$$I_1/I_2 = N_1/N_2 \quad (1)$$

where I_1 is the intensity (or number of counts) of the reference, I_2 is the intensity (or number of counts) of the surface, N_1 is the number of molecules of the reference, and N_2 is the number of molecules of the surface. The surface density (ρ) is defined as the ratio between the number of molecules on the surface and the modified area (A):

$$\rho = N/A \quad (2)$$

The average intermolecular distance (d) was calculated as

$$d = (1/\rho)^{1/2} \quad (3)$$

RESULTS AND DISCUSSION

Two methods of immobilizing oligonucleotides to glass were investigated: direct coupling of silanized DNA and indirect coupling through the biotin–streptavidin interaction. XPS, AFM, and radioactivity measurements and fluorescence imaging were used to characterize the resulting surfaces.

Immobilization of Silanized DNA. Direct coupling of silanized DNA to a surface has previously been shown to generate high surface DNA densities (20); oligonucleotides with thiol end groups are coupled in solution to mercaptosilane. The silanized DNA then binds selectively to the glass surface (Scheme 1a). AFM images of the unmodified glass surface are compared in Figure 1 with those from surfaces treated with the silanized DNA and mercaptosilane alone. Both modified surfaces showed an increase in roughness from an rms of 1.5 nm on the untreated glass to 5 nm on the treated surfaces. It is likely that the increased roughness was due to the development of multilayer islands of silane. Silanized surfaces are known to be prone to polymerization, and it is likely that this is responsible for the increased roughness observed here. However, silanization results in only a negligible attenuation of the K 2p photoemission peak at 292.5 eV binding energy (Figure 1d). Because the latter arises from a potassium component in the underlying glass substrate and the mean-free path of electrons at this kinetic energy is approximately 3 nm, we can infer that polymer growth does not significantly exceed this depth.

Scheme 1. (A) Immobilization of Silanized DNA Prepared by Mixing (3-Mercaptopropyl)trimethoxysilane with Thiol-Modified DNA Labeled with Atto488, (B) Immobilization by the Biotin–Streptavidin Interaction; Glass Modified with APTES Followed by NHS–Biotin, before Binding of Streptavidin, Biotinylated Probe, and Hybridization of the Labeled Target, and (C) Control of the Intermolecular Distance by Varying the Ratios between Two Different Probes Immobilized on the Surface

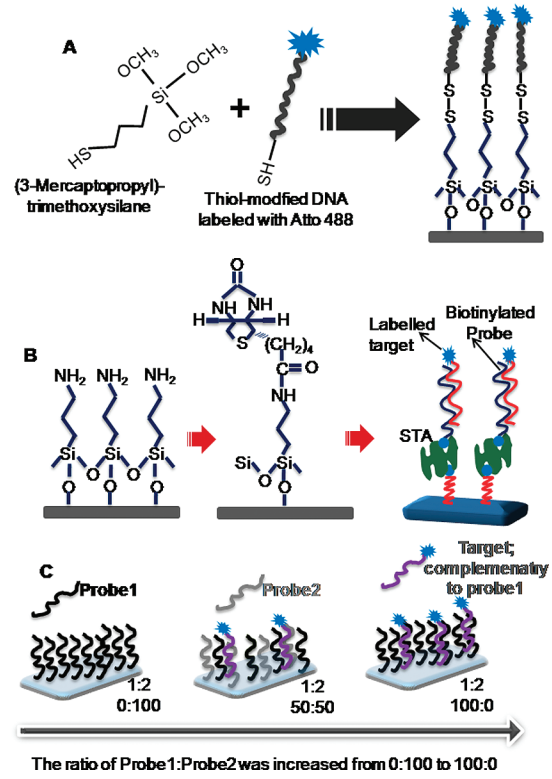

The XPS data also show the surface presence of the silanized DNA with a strong peak in the N 1s region (Figure 1e) and an increase in the intensity of the C 1s peak at 288 eV characteristic of carbons associated with electron-withdrawing groups such as nitrogen and oxygen. Quantification of the XPS data is hindered, however, by the roughness of the surface, which can lead to errors in surface concentration estimates. Radioactive measurements of thiol-modified, labeled DNA (Radio-Target; Table 1) indicated a nominal surface density in the range of 0.03–0.04 DNA molecules/nm^2, i.e., an intermolecular distance in the range of 5–6 nm. The surface density for thiol-modified, fluorescent, silanized oligonucleotides was quantified by fluorescence imaging, as shown in Figure 1f. In this case, the calculated surface density was in the range of 0.01–0.04 molecules/nm^2, which corresponds to an average intermolecular distance of 5–10 nm. The different methods were used several times for different samples to confirm the reproducibility of the surface immobilization; overall, the

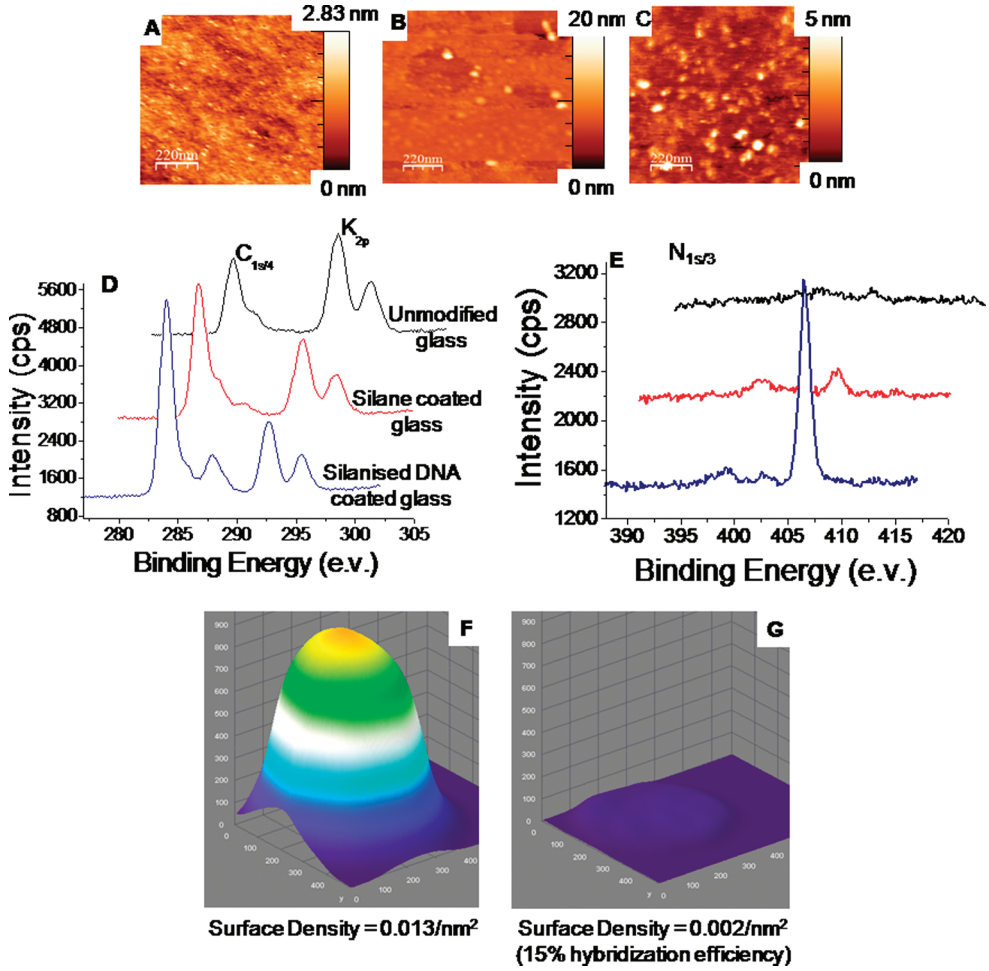

FIGURE 1. (A) AFM images of a clean glass surface. (B) Glass surface coated with silane. (C) Glass surface modified with silanized DNA. (D) XPS spectra of the C 1s region for clean glass, silanized glass, and silanized DNA-modified glass surfaces. Note the strong K 2p signal at ~292.5 eV due to a potassium component of the substrate. (E) XPS spectra of the N 1s region showing the strong peak due to the adsorption of silanized DNA on the glass surface. (F) Fluorescence image of the silanized DNA labeled with Atto488. (G) Fluorescence image of the surface after hybridization showing a very low hybridization efficiency.

surface densities as calculated by radioactive and fluorescence imaging were felt to be comparable based on the uncertainties in the absolute quantification associated with each technique. The surface accessibility was examined by DNA hybridization. Fluorescent-labeled oligonucleotides were hybridized to surfaces modified with unlabeled, complementary sequences. Figure 1g shows a fluorescent image after hybridization. The maximum surface density achieved was in the range of 0.002−0.006 molecules/nm^2, suggesting a hybridization efficiency of up to 15% relative to the primary coupled "anchor" oligonucleotides. Similar hybridization densities (0.003 molecules/nm^2) were obtained using radioactive measurements. Previous studies have suggested that steric interference with the silanized surface may interfere with hybridization and showed that additional "spacer" bases at the 5′ end of the oligonucleotide could raise the hybridization efficiency (30). On the basis of this hypothesis, we tried to hybridize a 15-mer complementary oligonucleotide to the last 15-mer of the silanized DNA. However, this did not improve the hybridization efficiency where it did not exceed the previously achieved value (15%). We also investigated hybridization times ranging from 30 min to 6 h; however, there was no significant increase in the surface hybridization efficiency (data not shown). We therefore concluded that, using silanized DNA, it was possible to prepare glass surfaces with a high density of immobilized DNA molecules but that the DNA was largely inaccessible for hybridization. We speculate that the low hybridization efficiency may be due to DNA physisorption of hybridization-accessible bases to the glass surface following covalent coupling of the 5′ base.

Immobilization of DNA by the Biotin−Streptavidin System. The second method used to immobilize the DNA to the glass surface involved the use of a streptavidin protein tetramer as a "sandwich" to link a biotinylated glass surface to biotinylated oligonucleotides (Scheme 1b). In this instance, the glass surface was first amino-modified using APTES prior to modification with NHS−biotin. The surface was then coated with streptavidin prior to the addition of biotinylated "anchor" oligonucleotides. Using streptavidin has potential advantages; it has at least two free binding sites that increase the possibility of the probe binding, and streptavidin is also thought to reduce nonspecific adsorption (31, 32). AFM imaging was performed for the clean glass and after application of APTES and NHS−biotin. Figure 2a shows

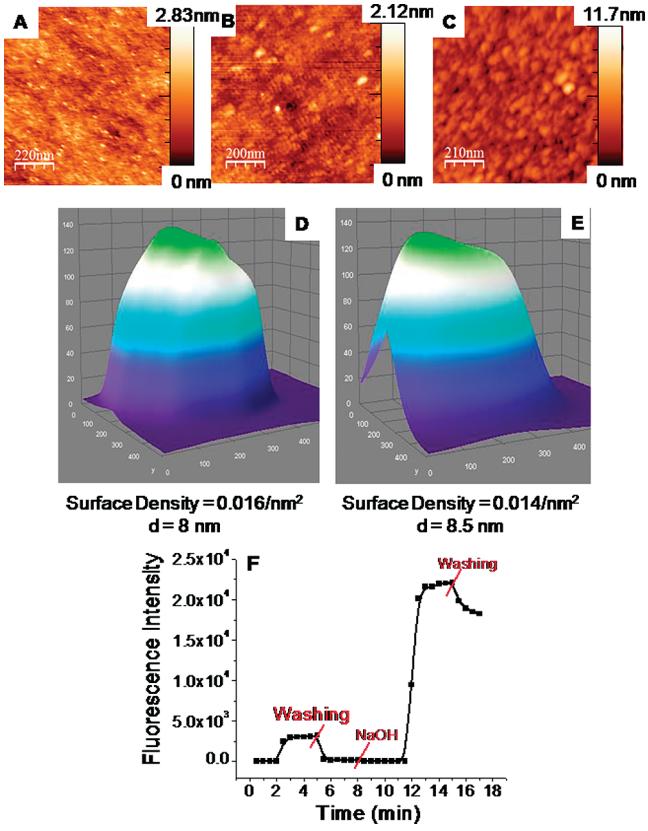

FIGURE 2. (A) AFM image of clean glass. (B) Glass modified with NHS−biotin. (C) Glass surface after coupling of streptavidin to NHS−biotin. (D) Fluorescence image of the surface after coupling of the biotinylated DNA labeled with Atto488 to streptavidin. (E) Fluorescence image of the surface after hybridization of the labeled target to a biotinylated probe. (F) Real-time TIR fluorescence measurements of a mismatch oligonucleotide as a control showing a very low signal and hybridization of 500 nM target showing a very strong binding signal.

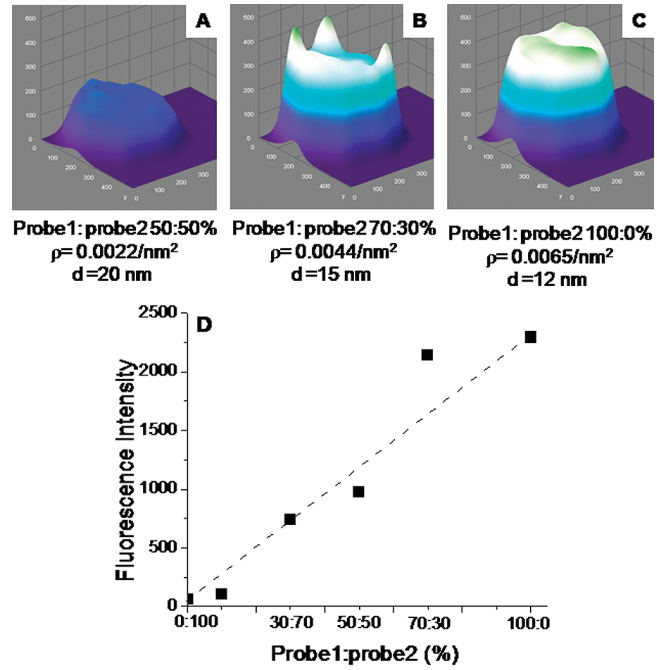

FIGURE 3. Fluorescence imaging of the hybridization of a labeled DNA oligonucleotide to three different samples with (A) a 50:50 ratio of biotinylated probe1:probe2, (B) 70:30, and (C) 100:0, showing the increase in the fluorescence intensity. (D) In situ TIR fluorescence measurements of the surface hybridization as a function of probe1: probe 2 ratios. The nonlinearity might correlate with a slight variation in the intensity on different areas on the surface as in part B.

the AFM image of the clean glass with a rms roughness of 1.5 nm. After application of APTES and NHS−biotin, the rms roughness was reduced to 0.65 nm. It is known that the APTES layer can have a surface thickness of 0.8 ± 0.1 nm (33). The value we determined for the APTES/NHS−biotin-modified surface suggested that gaps in the original glass surface may have been filled by the silane/biotin molecules to form a flat homogeneous layer. After application of streptavidin, the surface rms roughness was 3.2 nm, which is of an order similar to that of the dimensions of a streptavidin tetramer (~5 nm; Figure 2c). To quantify the surface density of biotinylated oligonucleotides, 500 nM biotinylated DNA labeled with Atto488 (Biotin-Target; Table 1) was applied to the surface prior to imaging. A surface density of 0.016 molecules/nm^2 was determined, corresponding to an intermolecular distance of 8 nm (Figure 2d). To examine surface accessibility, a biotinylated "anchor" oligonucleotide (Probe1; Table 1) was bound to the surface and was then hybridized to 500 nM complementary oligonucleotide labeled with Atto488 (Target; Table 1). After washing with PBS, a surface density of the hybridized target of 0.014 molecules/nm^2 was determined (Figure 2e). This equated to an average intermolecular distance of 8.5 nm and a hybridization efficiency of 90%. This high hybridization efficiency indicated very good surface accessibility and was comparable to the hybridized efficiency achieved on gold surfaces, which was 95% at low probe densities (13). Notice that this high hybridization efficiency was achieved with a fully complementary probe oligonucleotide and did not require the presence of "spacer bases" to increase the surface accessibility. One advantage of the biotin−streptavidin surface is that hybridized oligonucleotides (but not the biotinylated oligonucleotide) could be removed with a brief wash in 50 mM NaOH (34). This allowed repeated measurements to be made on the same surface using TIR in a flow-cell format. Time-lapse measurements were carried out during the batch injections of oligonucleotides and wash solutions. Figure 2f shows that the initial incubation of the surface with a noncomplementary oligonucleotide labeled with Atto488 as a control (Control Oligo; Table 1) gave rise to a low signal that was washed away by PBS. By contrast, the complementary labeled target gave a strong fluorescence signal that was stable after washing in PBS.

Intermolecular Distance Control. Control of the intermolecular distance between the DNA molecules was achieved by the immobilization of two different biotinylated "probe" or anchor oligonucleotides (Probe1 and Probe2) and hybridization of a target or hybrid oligonucleotide (Target 1) that was complementary to just Probe1 (Scheme 1c). Several samples were prepared with different Probe1:Probe2 ratios. Parts a−c of Figure 3 show the fluorescence images with a subset of Probe1:Probe2 ratios. Figure 3d, determined by in situ fluorescence measurements in the TIR mode, shows a clear relationship between the fluorescence intensity and the Probe1:Probe2

ratio. The increase in the fluorescence signal with an increase in the ratio of the complementary probe suggests that this method could be a useful way of controlling the surface density. The increase in the fluorescence intensity for some of the samples did not tightly fit with the oligonucleotide ratio. The primary reason for this variation was probably due to the lack of homogeneity in oligonucleotide coupling across the coupled surface area. For example, fluorescence images in Figure 1b show a level of nonhomogeneity across the surface. The fluorescence imaging collects the average signal over a wide imaged area, while the laser beam used in the TIR fluorescence optical setup was much smaller in size and was therefore more sensitive to local variations of the fluorescence intensity.

CONCLUSIONS

In this work, we successfully generated a uniform planar surface of oligonucleotides that was highly accessible for hybridization. Direct silanization and an indirect biotin−streptavidin technique were compared. An orthogonal mix of characterization methods, AFM, XPS, radioactivity, and fluorescence imaging, were shown to be required for a robust comparison of the surface modification methods. Both methods generated high surface oligonucleotide densities, but hybridization measurements clearly showed that the silanized DNA had low accessibility while biotin−streptavidin-coupled "anchor" oligonucleotides were highly accessible. Importantly, the biotin−streptavidin method did not generate rough surfaces at the 2−4 nm scale. We conclude that the biotin−streptavidin method is an appropriate technique where high levels of oligonucleotides need to be coupled on molecularly flat monolayer surfaces.

Acknowledgment. The authors thank the following colleagues who helped in this work: Basit Yameen from the Max Planck Institute for polymer Research, Mainz, Germany, for advice on surface chemistry, Jenita Bhantoo from Cardiff School of Chemistry for help with AFM imaging, David Morgan from Cardiff School of Chemistry for help with measurement and analysis of the XPS data, and Nick Kent and Jonathan Ryves for advice concerning the radioactivity work. The authors thank both Bjorn Persson from GE Healthcare and Prof. Elisabeth Hall from Cambridge University for useful discussions. This work was cofunded by the Technology Strategy Board.

REFERENCES AND NOTES

(1) Schulze, A.; Downward, J. *Nat. Cell Biol.* **2001**, *3*, E190–195.
(2) Woody, O. Z.; Doxey, A. C.; McConkey, B. J. *Evolut. Bioinform.* **2008**, *4*, 139–152.
(3) Rando, O. J. *Trends Genet.* **2007**, *23*, 67–73.
(4) Pollack, J. R.; Perou, C. M.; Alizadeh, A. A.; Eisen, M. B.; Pergamenschikov, A.; Williams, C. F.; Jeffrey, S. S.; Botstein, D.; Brown, P. O. *Nat. Genet.* **1999**, *23*, 41–46.
(5) Bignell, G. R.; Huang, J.; Greshock, J.; Watt, S.; Butler, A.; West, S.; Grigorova, M.; Jones, K. W.; Wei, W.; Stratton, M. R.; Futreal, P. A.; Weber, B.; Shapero, M. H.; Wooster, R. *Genome Res.* **2004**, *14*, 287–295.
(6) Zhao, X.; Pan, F.; Lu, J. R. *Annu. Rep. Prog. Chem., Sect. C: Phys. Chem.* **2007**, *103*, 261–286.
(7) Du, Q.; Larsson, O.; Swerdlow, H.; Liang, Z. *Top. Curr. Chem.* **2006**, *261*, 45–61.
(8) Babkina, S. S.; Budnikov, G. K. *J. Anal. Chem.* **2006**, *61*, 728–802.
(9) Haynie, D. T.; Qun, G. U.; Chuanding, C.; Suryanarayanan, S.; Dai, K. *Phys. E* **2006**, *33*, 92–98.
(10) Nikolelis, D. P.; Hianik, T.; Krull, U. J. *Electroanalysis* **1999**, *11*, 7–15.
(11) Cederquist, K. B.; Golightly, R. S.; Keating, C. D. *Langmuir* **2008**, *24*, 9162–9171.
(12) Preuss, M.; Bechstedt, F. *Surf. Sci.* **2008**, *602*, 1643–1694.
(13) Peterson, A. W.; Heaton, R. J.; Georgiadis, R. M. *Nucleic Acids Res.* **2001**, *29*, 5163–5168.
(14) Rogers, Y.; Jiang-Baucom, P.; Huang, Z.; Bogdanov, V.; Anderson, S.; Boyce-Jacino, M. T. *Anal. Biochem.* **1999**, *266*, 23–30.
(15) Chrisey, L. A.; Lee, G. U.; O'Ferrall, C. E. *Nucleic Acids Res.* **1996**, *24*, 3031–3093.
(16) Mahajan, S.; Kumar, P.; Gupta, K. C. *Bioconjugate Chem.* **2006**, *17*, 1184–1189.
(17) Ghosh, S. S.; Musso, G. F. *Nucleic Acids Res.* **1987**, *15*, 5353–5372.
(18) Guo, Z.; Guilfoyle, R. A.; Thiel, A. J.; Wang, R.; Smith, L. M. *Nucleic Acids Res.* **1994**, *22*, 5456–5465.
(19) Okamoto, A.; Tainaka, A.; Saito, I. *Tetrahedron Lett.* **2002**, *43*, 4581–4583.
(20) Kumar, A.; Larsson, O.; Parodi, D.; Liang, Z. *Nucleic Acids Res.* **2001**, *28*, e71–e71.
(21) Kwon, S. H.; Hong, B. J.; Park, H. Y.; Knoll, W.; Park, J. W. *J. Colloid Interface Sci.* **2007**, *308*, 325–331.
(22) Le Berre, V.; Trevisiol, E.; Dagkessamanskaia, A.; Sokol, S.; Caminade, A.; Majoral, J. P.; Meunier, B.; Francois, J. *Nucleic Acids Res.* **2003**, *31*, e88–e88.
(23) Liebermann, T.; Knoll, W. *Colloids Surf. A* **2000**, *171*, 115–130.
(24) Demirel, G.; Çağlayan, M. O.; Garipcan, B.; Pişkin, E. *Surf. Sci.* **2008**, *602*, 952–959.
(25) Dekeyser, C. M.; Buron, C. C.; Mc Evoya, K.; Dupont-Gillain, C. C.; Marchand-Brynaert, J.; Jonasc, A. M.; Rouxhet, P. G. *J. Colloid Interface Sci.* **2008**, *324*, 118–126.
(26) Vermeeren, V.; Wenmackers, S.; Daenen, M.; Haenen, K.; Williams, O. A.; Ameloot, M.; van de Ven, M.; Wagner, M.; Michiels, L. *Langmuir* **2008**, *24*, 9125–9134.
(27) Hamon, L.; Pastré, D.; Dupaigne, P.; Le Breton, C.; Le Cam, E.; Piétrement, O. *Nucleic Acids Res.* **2007**, *35*, e58–e58.
(28) Horcas, I.; Fernandez, R.; Gomez-Rodriguez, J.; Colchero, J.; Gomez-Herrero, J.; Baro, A. *Rev. Sci. Instrum.* **2007**, *78*, 013705–013708.
(29) Carley, A. F.; Roberts, M. *Proc. R. Soc. London, Ser. A* **1978**, *363*, 403–424.
(30) Guo, Z.; Guilfoyle, R. A.; Thiel, A. J.; Wang, R.; Smith, L. M. *Nucleic Acids Res.* **1994**, *22*, 5456–5465.
(31) Ando, T.; Uchihashi, T.; Fukuma, T. *Prog. Surf. Sci.* **2008**, *83*, 337–437.
(32) Lee, H.; Kim, T. H.; Park, T. G. *J. Controlled Release* **2002**, *83*, 109–119.
(33) Libertino, S.; Giannazzo, F.; Aiello, V.; Scandurra, A.; Sinatra, F.; Renis, M.; Fichera, M. *Langmuir* **2008**, *24*, 1965–1972.
(34) Yao, D. F.; Kim, J.; Yu, F.; Nielsen, P. E.; Sinner, E. K.; Knoll, W. *Biophys. J.* **2005**, *88*, 2745–2571.

AM9003073